

# Bump Hunting in Latent Space

Blaž Bortolato\* and Aleks Smolkovič†  
*Jožef Stefan Institute, Jamova 39, 1000 Ljubljana, Slovenia*

Barry M. Dillon‡  
*Institut für Theoretische Physik, Universität Heidelberg, Germany*

Jernej F. Kamenik§  
*Jožef Stefan Institute, Jamova 39, 1000 Ljubljana, Slovenia and  
 Faculty of Mathematics and Physics, University of Ljubljana, Jadranska 19, 1000 Ljubljana, Slovenia*  
 (Dated: March 1, 2025)

Unsupervised anomaly detection could be crucial in future analyses searching for rare phenomena in large datasets, as for example collected at the LHC. To this end, we introduce a physics inspired variational autoencoder (VAE) architecture which performs competitively and robustly on the LHC Olympics Machine Learning Challenge datasets. We demonstrate how embedding some physical observables directly into the VAE latent space, while at the same time keeping the classifier manifestly agnostic to them, can help to identify and characterise features in measured spectra as caused by the presence of anomalies in a dataset.

**Introduction** The absence of new physics (NP) discoveries thus far at the LHC strains many of the scenarios beyond the standard model (BSM) put forward in the last decades to address the theoretical and phenomenological weaknesses of the SM. It is possible that NP is present at mass scales just out of reach of the LHC, in which case effective field theory methods may help infer the presence of structures in the low-statistics tails of distributions measured at the LHC. Another possibility however is that new degrees of freedom are already being produced at the LHC, but that existing search strategies have not been specific enough to disentangle their signatures from the backgrounds. In going beyond the most motivated NP scenarios it becomes impractical to consider searching for all possible signatures. To address this problem, unsupervised machine learning tools can be used to search for NP signals with no a-priori knowledge on what the relevant signatures may be. In particular, *anomaly detection* techniques address the problem of searching for rare a-priori unknown signals in isolated regions of measured phase-space. Several classes of unsupervised methods using Deep Neural Networks (DNNs) have been explored in the literature thus far; CWoLa-based methods [1–6]<sup>1</sup>, autoencoder (AE) and variational AE (VAE) based methods [8–16], and others [17–23]. However visualising what has been learned by a DNN is notoriously difficult<sup>2</sup>. In this Letter we introduce a novel VAE architecture and optimization strategy to address two general outstanding

issues in unsupervised VAE methods for (di-jet) anomaly detection: (i) robustness of anomaly detection performance, and (ii) physical characterisation of the VAE latent space (i.e. with respect to the invariant mass of the di-jet events).

**Dataset and Observables** We demonstrate our approach using the LHC Olympics R&D dataset [29], consisting of  $10^6$  simulated QCD di-jet events and up to  $10^5$   $Z' \rightarrow X(\rightarrow q\bar{q})Y(\rightarrow q\bar{q})$  events with  $m_{Z'} = 3.5$  TeV,  $m_X = 500$  GeV and  $m_Y = 100$  GeV. Details on the simulation and kinematic cuts can be found in the reference. From each event we select the two jets with the highest  $p_T$  and then order them by their mass in the input layer of the VAE. For reasons of generality, we only use a small set of standard high-level observables in the analysis:<sup>3</sup> the jet mass ( $m_j$ ) and two ratios of N-subjettiness observables ( $\tau_2/\tau_1, \tau_3/\tau_2$ ) for each jet [31]. For our chosen set of observables the signal events differ significantly from background in just the mass of the heaviest jet and  $\tau_1/\tau_2$  of both jets. Whereas the  $\tau_3/\tau_2$  distributions do not exhibit distinguishing characteristics. This is realistic since in a typical model-agnostic BSM search we would expect only a subset of the observables to be sensitive to the signal.

Using the VAE we want to obtain a classification score for each event, indicating how signal- or background-like the event is, which can then be used in a search for a localised excess (i.e. a *bump hunt*) in the di-jet invariant mass ( $m_{jj}$ ) spectrum of the events. Importantly in this approach, the di-jet invariant mass observable itself should not be among the inputs to the VAE, nor should it

\* Electronic address: [blaz.bortolato@ijs.si](mailto:blaz.bortolato@ijs.si)

† Electronic address: [aleks.smolkovic@ijs.si](mailto:aleks.smolkovic@ijs.si)

‡ Electronic address: [dillon@thphys.uni-heidelberg.de](mailto:dillon@thphys.uni-heidelberg.de)

§ Electronic address: [jernej.kamenik@cern.ch](mailto:jernej.kamenik@cern.ch)

<sup>1</sup> Most notably, the ATLAS collaboration has recently implemented a CWoLa-based weakly supervised di-jet search [7].

<sup>2</sup> Another class of unsupervised techniques based on Latent Dirichlet Allocation (LDA) [24–26] and other topic modelling methods [27, 28] do provide interpretability, but are not based on DNNs.

<sup>3</sup> Observables more specially suited for the LHC Olympics data have been previously considered and can in principle result in further significant increases in performance for a specific dataset, albeit at the price of potential loss of generality, see e.g. Ref. [30].

be directly computable from the inputs, since this would introduce classification bias (i.e. sculpting) in the bump hunt analysis (see e.g. Ref. [32] for a more detailed discussion).

Finally, data pre-processing can have drastic effects on the classification performance, the stability, and the early stopping conditions. We tested our method using different data pre-processing schemes available in the `scikit-learn` v0.23.2 library [33]. We found that using the common `MaxAbsScaler` works well for our choice of observables, however we emphasise that this step should be handled with care, depending on the observables' distributions in a given dataset.

**VAE Architecture and Training** The VAE architecture [34] and loss function define a probabilistic model for the di-jet data in which each event can be described by a single latent variable  $z$ . The function  $p(z|\text{event})$  is the posterior distribution and encodes information on the latent structure of that event. As shown on the upper scheme on Fig. 1, the VAE consists of two components, an encoder and a decoder, where the encoder models the posterior distribution for the model  $p(z|\text{event})$  and the decoder models the likelihood  $p(\text{event}|z)$ . The encoder consists of a neural network mapping each event to a mean  $\bar{z}$  and a log variance  $\log \sigma_z^2$ , and a sampling step in which a value  $z$  is sampled from a Gaussian distribution parameterized by  $\bar{z}$  and  $\log \sigma_z^2$ . The decoder consists of a neural network mapping the value  $z$  back to a reconstructed event. Together this sequence defines a single forward pass through the VAE. A key feature here is the bottleneck  $z$ , i.e. the latent space, which is a compressed representation of the event from which the decoder must attempt to reconstruct the full event. Note that for a severely compressed (low dimensional) latent space one does not expect the VAE to accurately reconstruct individual events, nor all the observable distributions. However, the medians of these distributions are expected to be learned most easily and thus reconstructed most accurately.

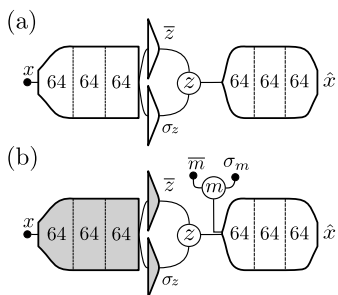


Figure 1. The standard VAE architecture (a) and the decoder re-training step (b), where the weights of the grayed out nodes are fixed. See text for details.

The weights and biases of the VAE are optimised such that the Evidence-Lower-BOund (ELBO) of the probabilistic model evaluated on the dataset is maximised. This ELBO consists of two terms, the reconstruction loss

and the KL-divergence with respect to the normal prior in latent space, with the latter acting as a regulariser on the latent space distribution of events. In general the two terms can be weighted differently relative to each other, which in the end relates to the variance on the reconstructed events produced on the output layer of the decoder [35]. The resulting loss function can be expressed as

$$\mathcal{L} = -\alpha \log p(\text{event}|z) - \frac{1}{2} (1 + \log \sigma_z^2 - \bar{z}^2 - \sigma_z^2), \quad (1)$$

where  $-\log p(\text{event}|z)$  is modelled by the mean-squared-error between the input and output events, and the second term arises from the KL divergence between the posterior distribution for a single event and the Normal distribution. Consistent with previous studies, we find that  $\alpha \in [10^3, 10^4]$  results in good performance and avoids s.c. ‘component collapse’ in which the KL divergence forces the means and log variances of all events to 0. For definiteness, in the following we present results for a value of  $\alpha = 5000$ , however, our results were found not to be sensitive to  $\mathcal{O}(1)$  changes in  $\alpha$ .

The weights and biases of the networks were trained via back-propagation with the following architecture: 3 hidden layers with 64 nodes and SeLU activations were used in both the encoder and the decoder, with the output layers of both having linear activations. Our final results are however insensitive to small changes in the choice of the DNN architecture or training parameters. All of the numerical procedures were implemented with `TensorFlow` v2.3.1 [36].<sup>4</sup> After an extensive study of optimisation techniques we found the best results using the Adadelata optimizer [37]. In particular, training with the more widely used Adam [38] optimiser (with default hyper-parameters) performed poorly and with less stability. This is possibly due to the momentum feature, i.e. the adaptive estimation of first and second order moments, which is designed specifically to increase the speed of training by reducing sensitivity to outliers in the data. The Adadelata optimiser on the other hand uses adaptive learning rates per-dimension, and aims to prevent the continuous decay of learning rates throughout the training while allowing the network to determine the learning rates on the fly. For an in-depth comparison of different optimisers, see Ref. [39]. In our analysis the networks were trained using a batch size of 1000 for up to a maximum of 100 epochs.

Traditionally the reconstruction loss has been used as a classification metric with autoencoders and even VAEs. However we find that for anomaly detection this is never a good metric, in agreement with other recent studies in high-energy physics [16, 40]. Instead we find that classification metrics derived from the latent space representation of the events are much more performant and stable.

<sup>4</sup> The code is publicly available at <https://github.com/alekssmolnikov/BuHuLaSpa>

In particular we find that the KL divergence between the latent space representation of an event and the prior distribution is a consistently good classifier. However there is a drawback. Because the optimisation goal of the VAE is not aligned with the classification goal, the training typically reaches a point after which the classification performance of the latent space metrics degrade. This is highly correlated with a peak in the KL loss term, and is likely due to an over-regularisation from this term once the reconstruction loss becomes very small.<sup>5</sup> Our solution is to terminate the training at the epoch where this KL loss is largest, and then use the latent space representation of the events at this epoch for classification.

**Classification results** We consider 3 values of  $S/B \in [10\%, 1\%, 0.1\%]$  and for each train 20 models. The training for each model is terminated once the KL loss peaks and the network at the epoch of largest KL loss is used for classification. For robustness we ensemble the output of the encoders in each of the 20 runs per  $S/B$ , using the mean of the per-event KL divergence as the classifier. The performance of such a classifier at  $S/B = 0.1\%$  is shown with a black line on Fig. 2, with the signal and background distributions of the average per-event KL shown in the inset plot. The uncertainty on the classification, indicated by the blue region around the ROC curve, is estimated using the standard deviation of the per-event KL divergences around the mean. We do not show the results for larger  $S/B$ , however the only considerable difference is that the width of the blue band narrows for larger  $S/B$ . Note that this classifier is able to improve significance ( $S/\sqrt{B}$ ) of the signal in the given dataset by up to a factor of almost three. Since it does not employ sidebands nor signal region scanning, it is free from trials factors associated with such techniques.

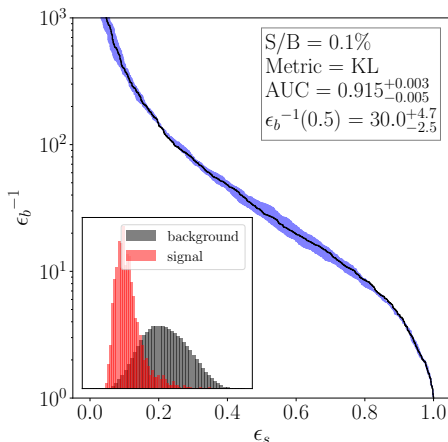


Figure 2. ROC performance on the LHC Olympics test data with  $S/B = 0.1\%$ . See text for details.

<sup>5</sup> This is also related to the choice of  $\alpha$  discussed previously.

**Latent Space Characterisation** VAEs are generative models and from the latent space representation of the data they learn a likelihood function parameterised by the decoder. We can use this decoder to test how well the VAE is encoding data in the latent space. One of the unique features of the VAE set-up so far is the use of the Adadelta optimiser, which is crucial for obtaining good classification performance. However we find that we actually obtain better reconstructions of the data by re-training only the decoder using the Adam optimiser. This makes sense, since the drawback of Adam in training the VAE is associated with the momentum feature smoothing over outliers in the training data, in the generation step this is not an issue. Also, in the re-training step contrary to the initial VAE training, we can now train the decoder until approximate convergence (typically after few tens of epochs).

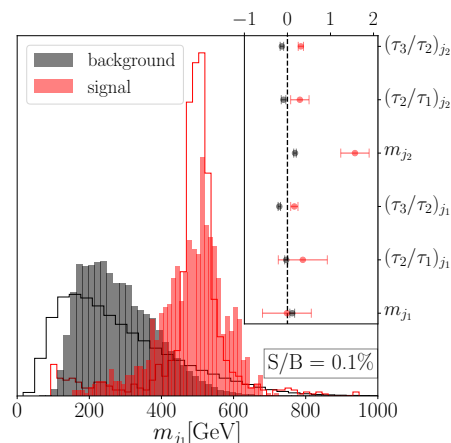


Figure 3. Input (outline) and reconstructed (filled) leading jet mass distribution for both signal and background, with the inset plot showing the difference between medians of the input and reconstructed distributions, normalized to the standard deviations of the input distributions. See text for details.

The re-training of the decoder allows us to introduce an additional mechanism to enhance the physical characterisation of the latent space. We can explicitly embed the invariant mass observable for each event as a direction in latent space orthogonal to the 1D  $z$  direction, as depicted on the lower scheme on Fig. 1. This is done by an additional sampling of  $m_{jj}$  from a Gaussian distribution centred at the measured invariant mass of the di-jet event,  $\bar{m} = m_{jj}$  with a standard deviation of  $\sigma_m = 0.025 \times m_{jj}$ , corresponding to an approximate 5% error on the invariant mass observable. To make the invariant masses more compatible with the  $z$  inputs in the decoder, they are rescaled using the **StandardScaler** (along with the appropriate rescaling of the sampling standard deviations). Note that, since in the re-training step, the encoder is frozen, the classifier remains agnostic to  $m_{jj}$ . In Fig. 3 we plot the reconstruction of the leading jet mass for both signal and background, while in the inset figure we plot the difference between the median of the reconstructed

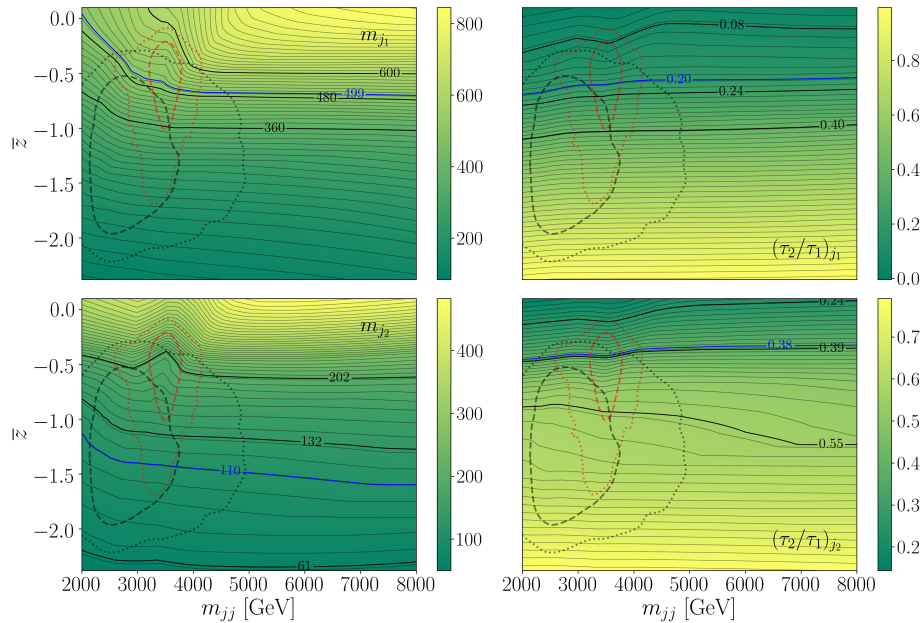


Figure 4. Generated jet observables  $(m_j, \tau_2/\tau_1)$  produced by scanning over the latent space observables  $(z, m_{jj})$  in a network trained with  $S/B = 1\%$ . The range in  $z$  is determined by the range of  $\bar{z}$  produced by the encoder network. For each feature the solid black contours denote the values of the true signal mean and one standard deviation around it, while the solid blue contour shows the value of the median. The dashed and dotted contours show the regions in the latent space in which 68% and 95% of signal (red) and background (black) resides.

distribution and the median of the input distribution for each observable, normalized by the standard deviation of the input distribution. Despite having just  $S/B = 0.1\%$  the network is clearly able to reconstruct the leading jet mass for both signal and background, and reconstructs all other observables' medians adequately with the exception of the lighter jet mass, which is almost  $2\sigma$  away from its input value.

The latent space now consists of  $z$  and  $m_{jj}$ , so we can generate observables' distributions by performing a 2D scan over the latent space using the generative model (the decoder) as a function of the invariant mass of the events and a latent variable  $z$ . This allows to characterise the latent space in terms of physical observables as a function of the invariant mass. At the same time the classifier (the encoder) remains invariant mass agnostic and maps each event to a posterior distribution over  $z$  only. In Fig. 4 we scan  $(z, m_{jj})$  plotting the generated jet masses and  $\tau_2/\tau_1$  observables for the VAE trained on the LHC0 test data with  $S/B = 1\%$ . Here we can clearly see the defects imprinted on the latent space from the anomalous di-jet events at invariant masses around 3.5 TeV. At lower  $S/B$  the localised features in the invariant mass become undetectable, however this method nevertheless provides a direct insight into what physics is being encoded in the VAE latent space. We have also checked explicitly that training the VAE on background only events does not introduce spurious localized features in the invariant mass distributions of observables generated by the decoder.

**Outlook** In this Letter we have introduced a novel anomaly detection and characterisation approach using a two-step VAE architecture, and demonstrated its performance and robustness on the LHC Olympics R&D dataset, (we also applied it successfully to the Black Box 1 dataset, where it compares favourably to other existing anomaly detection approaches, see Ref. [30]). Our method is however general and can easily be applied to other physics datasets beyond LHC di-jet spectra. Contrary to known existing approaches, neither the classification nor the characterisation step rely on assumptions about the signal shape or presence of predefined sidebands. It can also be refined in several directions using e.g. larger latent space representations of both the encoded observables used for classification, as well as scanning observables used in the bump-hunting or characterisation step, particularly with the goal of increasing the sensitivity of the physical latent space characterisation to smaller  $S/B$  ratios, as well as improving the observables' reconstruction accuracy. To conclude, our results demonstrate how combining physics concepts with modern ML techniques can enhance our understanding of rare signals in large datasets and potentially help to uncover unexpected new physics.

**Acknowledgements** The authors thank Andrej Matvec for his involvement in the initial stages of the project. BB, JFK and AS acknowledge the financial support from the Slovenian Research Agency (research core funding No. P1-0035). BD acknowledges funding from BMBF.

- 
- [1] E. M. Metodiev, B. Nachman and J. Thaler, *Classification without labels: Learning from mixed samples in high energy physics*, *JHEP* **10** (2017) 174, [[1708.02949](#)].
- [2] J. H. Collins, K. Howe and B. Nachman, *Anomaly Detection for Resonant New Physics with Machine Learning*, *Phys. Rev. Lett.* **121** (2018) 241803, [[1805.02664](#)].
- [3] J. H. Collins, K. Howe and B. Nachman, *Extending the search for new resonances with machine learning*, *Phys. Rev.* **D99** (2019) 014038, [[1902.02634](#)].
- [4] K. Benkendorfer, L. L. Pottier and B. Nachman, *Simulation-Assisted Decorrelation for Resonant Anomaly Detection*, [2009.02205](#).
- [5] O. Amram and C. M. Suarez, *Tag N' Train: A Technique to Train Improved Classifiers on Unlabeled Data*, [2002.12376](#).
- [6] A. Andreassen, B. Nachman and D. Shih, *Simulation Assisted Likelihood-free Anomaly Detection*, [2001.05001](#).
- [7] ATLAS Collaboration, *Dijet resonance search with weak supervision using 13 TeV pp collisions in the ATLAS detector*, [2005.02983](#).
- [8] M. Farina, Y. Nakai and D. Shih, *Searching for New Physics with Deep Autoencoders*, [1808.08992](#).
- [9] T. Heimel, G. Kasieczka, T. Plehn and J. M. Thompson, *QCD or What?*, *SciPost Phys.* **6** (2019) 030, [[1808.08979](#)].
- [10] T. S. Roy and A. H. Vijay, *A robust anomaly finder based on autoencoder*, [1903.02032](#).
- [11] J. Hajer, Y.-Y. Li, T. Liu and H. Wang, *Novelty Detection Meets Collider Physics*, [1807.10261](#).
- [12] M. C. Romao, N. Castro and R. Pedro, *Finding New Physics without learning about it: Anomaly Detection as a tool for Searches at Colliders*, [2006.05432](#).
- [13] S. Alexander, S. Gleyzer, H. Parul, P. Reddy, M. W. Toomey, E. Usai et al., *Decoding Dark Matter Substructure without Supervision*, [2008.12731](#).
- [14] A. Blance, M. Spannowsky and P. Waite, *Adversarially-trained autoencoders for robust unsupervised new physics searches*, *JHEP* **10** (2019) 047, [[1905.10384](#)].
- [15] O. Cerri, T. Q. Nguyen, M. Pierini, M. Spiropulu and J.-R. Vlimant, *Variational Autoencoders for New Physics Mining at the Large Hadron Collider*, [1811.10276](#).
- [16] T. Cheng, J.-F. Arguin, J. Leissner-Martin, J. Pilette and T. Golling, *Variational Autoencoders for Anomalous Jet Tagging*, [2007.01850](#).
- [17] J. A. Aguilar-Saavedra, J. H. Collins and R. K. Mishra, *A generic anti-QCD jet tagger*, *JHEP* **11** (2017) 163, [[1709.01087](#)].
- [18] B. Nachman and D. Shih, *Anomaly Detection with Density Estimation*, [2001.04990](#).
- [19] V. Mikuni and F. Canelli, *UCluster: Unsupervised clustering for collider physics*, [2010.07106](#).
- [20] M. van Beekveld, S. Caron, L. Hendriks, P. Jackson, A. Leinweber, S. Otten et al., *Combining outlier analysis algorithms to identify new physics at the LHC*, [2010.07940](#).
- [21] O. Knapp, G. Dissertori, O. Cerri, T. Q. Nguyen, J.-R. Vlimant and M. Pierini, *Adversarially Learned Anomaly Detection on CMS Open Data: re-discovering the top quark*, [2005.01598](#).
- [22] C. K. Khosa and V. Sanz, *Anomaly Awareness*, [2007.14462](#).
- [23] S. E. Park, D. Rankin, S.-M. Udrescu, M. Yunus and P. Harris, *Quasi Anomalous Knowledge: Searching for new physics with embedded knowledge*, [2011.03550](#).
- [24] B. M. Dillon, D. A. Faroughy and J. F. Kamenik, *Uncovering latent jet substructure*, *Phys. Rev.* **D100** (2019) 056002, [[1904.04200](#)].
- [25] B. M. Dillon, D. A. Faroughy, J. F. Kamenik and M. Szwec, *Learning the latent structure of collider events*, *JHEP* **10** (2020) 206, [[2005.12319](#)].
- [26] D. M. Blei, A. Y. Ng, M. I. Jordan and J. Lafferty, *Latent dirichlet allocation*, *Journal of Machine Learning Research* **3** (2003) 2003.
- [27] E. M. Metodiev and J. Thaler, *Jet Topics: Disentangling Quarks and Gluons at Colliders*, *Phys. Rev. Lett.* **120** (2018) 241602, [[1802.00008](#)].
- [28] E. Alvarez, F. Lamagna and M. Szwec, *Topic Model for four-top at the LHC*, *JHEP* **01** (2020) 049, [[1911.09699](#)].
- [29] D. S. G. Kasieczka, B. Nachman, “R&D Dataset for LHC Olympics Anomaly Detection Challenge, Apr., 2019.” DOI: 10.5281/zenodo.2629073.
- [30] G. Kasieczka et al., *The LHC Olympics 2020: A Community Challenge for Anomaly Detection in High Energy Physics*, [2101.08320](#).
- [31] J. Thaler and K. Van Tilburg, *Identifying boosted objects with n-subjettiness*, *Journal of High Energy Physics* **2011** (Mar, 2011) .
- [32] G. Kasieczka and D. Shih, *DisCo Fever: Robust Networks Through Distance Correlation*, [2001.05310](#).
- [33] F. Pedregosa, G. Varoquaux, A. Gramfort, V. Michel, B. Thirion, O. Grisel et al., *Scikit-learn: Machine learning in Python*, *Journal of Machine Learning Research* **12** (2011) 2825–2830.
- [34] D. P. Kingma and M. Welling, *Auto-encoding variational bayes*, [1312.6114](#).
- [35] A. A. Pol, V. Berger, G. Cerminara, C. Germain and M. Pierini, *Anomaly detection with conditional variational autoencoders*, 2020.
- [36] M. Abadi, P. Barham, J. Chen, Z. Chen, A. Davis, J. Dean et al., *Tensorflow: A system for large-scale machine learning*, in *12th {USENIX} Symposium on Operating Systems Design and Implementation ({OSDI} 16)*, pp. 265–283, 2016.
- [37] M. D. Zeiler, *Adadelata: An adaptive learning rate method*, [1212.5701](#).
- [38] D. P. Kingma and J. Ba, *Adam: A method for stochastic optimization*, [1412.6980](#).
- [39] D. Choi, C. J. Shallue, Z. Nado, J. Lee, C. J. Maddison and G. E. Dahl, *On empirical comparisons of optimizers for deep learning*, *CoRR* **abs/1910.05446** (2019) , [[1910.05446](#)].
- [40] J. Batson, C. G. Haaf, Y. Kahn and D. A. Roberts, *Topological obstructions to autoencoding*, 2021.